Sensors and Actuators B 180 (2013) 114–121

Contents lists available at SciVerse ScienceDirect

Sensors and Actuators B: Chemical

journal homepage: www.elsevier.com/locate/snb

Active surface tension driven micropump using droplet/meniscus pressure gradient

Roxana Shabani [a], Hyoung J. Cho [a,b,*]

[a] Department of Mechanical, Materials and Aerospace Engineering, University of Central Florida, Orlando, FL 32816-2450, USA
[b] School of Advanced Materials Science and Engineering, Sungkyunkwan University, Suwon 440-746, Republic of Korea

ARTICLE INFO

Article history:
Available online 29 May 2012

Keywords:
Micropump
Microvalve
Electrowetting on dielectric
Droplet
Surface tension
Contact angle

ABSTRACT

An active micropump with a simple layout and no moving parts is designed and fabricated which has on demand flow on/off capability. The micropump is based on droplet/meniscus pressure gradient generated by electrowetting on dielectric (EWOD). By altering the contact angle between liquid and solid using an electric field a pressure gradient was induced and a small droplet was pumped into the channel via a uniform flow rate. A surface tension based propellant method was introduced as a low power consumption actuation method in microfluidic devices. The liquid contact angle on the EWOD substrate was measured vs. electric potential and was used to obtain the capacitance of the substrate by fitting Young–Lippmann's equation. The capacitance of the EWOD substrate was also calculated to be $10 \pm 0.6\,\mu F/m^2$ by measuring the dielectric layer thickness which showed excellent agreement with the former method. EWOD setup parameters such as capacitance, saturation contact angle, hysteresis contact angle and onset voltage were discussed. A coupled theoretical–experimental model was developed to predict how much voltage is needed to start the micropump for different droplet sizes. The modeling results revealed that for droplets with a radius smaller than 0.4 mm the droplet will start going into the channel even when no voltage is applied. For any larger droplet, a certain voltage is needed to start the pump. It was also shown that decreasing the size of the input droplet and increasing the voltage will result in an increase in the pump flow. A model for describing the shrinkage of the micropump input droplet was developed, based on direct observations, which was in agreement with the forced wetting described in literature. This model was compared to the other models used to describe passively pumped droplets and evaporating microdrops.

1. Introduction

Micropumps and microvalves are the key components in handling small amount of aqueous samples [1–3]. Their importance is recognized, especially, in the field of analytical chemistry, biology and medicine in which massive and parallel screening of aliquots with the limited amount of usable samples is to be performed or a limited amount of dose needs to be supplied with good accuracy. In such applications, small amounts of biological samples or chemical reagents are introduced and transferred to analytical units by means of micropumps and microvalves, followed by chemical reactions and biochemical processes such as immobilization, labeling and detection [4,5]. Micropumps have been categorized by means of actuation methods applied to drive the flow rate. The electrostatic, piezoelectric, bimetallic, electroosmotic and electrowetting (EW) actuation methods have been reported [6].

The performance characteristics of micropumps for biological and chemical applications depend on critical parameters such as power consumption, flow rate, biocompatibility, disposability and durability of mechanical moving parts. Micropumps consisting of moving parts such as mechanical valves and membranes for controlling or actuating the liquid may be prone to mechanical failure, and their complicated structure and associated fabrication cost are prohibitive to integration [7]. Micropumps with low fabrication cost and minimal mechanical complexity are highly desirable for designing disposable biochips which could be easily replaced once the sample analysis is completed [8]. Therefore design and fabrication methods of micropumps with no moving parts are one of the central points of research in the field.

Among various actuation techniques, the surface tension-driven method was shown to be well suited for droplet based transport devices due to its favorable scaling effect [8–10].

The surface tension force is linearly proportional to the length of the interfacial line between the liquid, air and the solid (wetting line) in which a droplet forms the boundaries of the wetting

* Corresponding author at: Department of Mechanical, Materials & Aerospace Engineering, 4000 Central Florida Boulevard, University of Central Florida, Orlando, FL 32816-2450, USA. Tel.: +1 407 823 5014; fax: +1 407 823 0208.
E-mail address: hjcho@ucf.edu (H.J. Cho).

0925-4005/$ – see front matter © 2012 Elsevier B.V. All rights reserved.
http://dx.doi.org/10.1016/j.snb.2012.05.058

area on the solid surface. By scaling down the size of the system homogenously, the surface to volume ratio of the system increases and the surface forces which are negligible on macroscale become dominant on the microscale.

Although passive surface tension based micropumps are shown to be suitable for many applications [8,9], the ability to control the surface wettability to induce and stop the flow on demand would be highly desirable. The control of surface tension, by a temperature gradient in thermocapillary and by an electric potential gradient in electrocapillary, is implemented for micropumping [2,3]. However, electrocapillary in the forms of EW and EWOD are considered more power efficient than the thermocapillary [4]. EWOD is the most promising method due to the electrochemical inertness of the substrate and the ability to work with the non-electrolyte aqueous solutions. In EWOD phenomenon, the wetting properties of a hydrophobic surface could be modified by applying an electric field without changing the chemical composition of the surface.

Although EW and EWOD have been actively studied for a discrete droplet manipulation [11–14], to our knowledge an active micropump for continuous flows which takes advantage of EWOD has not been reported. The alteration of wettability as a propellant method could be combined with a valve to form a pump. However, the design and fabrication of a valve that could work with the actuating method and form a complete device remains challenging [1,15]. Most of the developed active electrical microvalves are driven by mechanical actuators [16]. In the proposed micropump, the flow could be turned on and off by switching the voltage on and off. On contrary to the previous works which used active mechanical microvalves for pumping, our device does not require any moving parts and is driven purely based on wettability of the surface which is altered by the electric potential. The key concept in our device is the linkage of this wettability control and the droplet/meniscus pressure gradient as a propellant method for driving a liquid in a microchannel. The power consumption is expected to be very small due to a very small current (<0.01 mA) associated with EWOD.

The biocompatibility imposes a limit on the type of the liquids which could be used for actuation in biomedical devices or induced chemical reactions. Although secondary transport liquid has been suggested as a solution for pumping water based solutions [16], the prevention of two liquids from mixing has remained an issue. Using the proposed micropump, aqueous solutions can be driven without using any electrolyte or secondary medium.

The EWOD micropump with its simple design could be used as a sample loading component in a disposable biochip. For example, it could be used to substitute syringe pumps for injecting samples into the plasma separators. Syringe pump is commonly used to fill the plasma separators with a sample [17–23]. Substituting it with a small scale disposable micropump is especially important when small amount of a sample needs to be used such as a blood sample or expensive chemical samples. The EWOD micropump could be easily integrated with the reported blood plasma separators in literature. The separators based on the Zweifach–Fung effect [17–19], geometric singularities [20], or large output channel [21,22], indicate the modular integration with the proposed pump is possible.

2. Materials, design and fabrication

The idea of the micropump was developed by direct observation of alteration of a water droplet's contact angle on hydrophilic surfaces such as glass or a silicon wafer with a native oxide layer, and hydrophobic surfaces such as a bare silicon wafer, fluorinated surfaces, or polydimethylsiloxane (PDMS) layers. The droplets with different contact angles would have different Laplace pressures due to the difference in their surface curvatures. A pressure gradient could be induced by altering the liquid contact angle on solid surface. As a low power consumption method for controlling the hydrophobicity of the solids and therefore inducing a pressure gradient, EWOD was employed. The EWOD-based micropump could be turned on and off on demand without any mechanical part and could work with non-electrolyte aqueous solutions.

In designing the micropump, it is assumed that the liquid of interest is applied in the form of a droplet using pipettes and syringes, which is a common protocol in chemistry. The size of the micropump is designed to work best with sample volumes on the microliter scale. The micropump chambers and channels are cast in biocompatible PDMS layer with low cost and simple fabrication process for disposability. PDMS is widely used in biological diagnosis lab on a chip in which transparency is required for optical measurement [24]. A single PDMS film is used both as bonding layer to the PDMS layer with a microchannel and the hydrophobic layer of the EWOD substrate. There are also other novelties in the fabrication process such as using spin on glass (SOG) as the insulating layer that could be applied in a very short time in compare to normally used dielectric layers in EWOD devices such as silicon dioxide.

2.1. EWOD substrate

The EWOD substrate of the micropump consists of a conductive layer which is used as the bottom electrode and a dielectric layer which insulates the liquid from the bottom electrode. A hydrophobic layer is formed on top of the insulating layer to put the meniscus in a non-wetting state before applying the voltage. A silicon wafer was used as the conductive layer. Other conductive substrates such as indium tin oxide (ITO) coated glass slides may also be used as the bottom electrode when a direct optical observation through the substrates is needed.

The electrical insulation was tested with both non-electrolyte and electrolyte aqueous solutions. The PDMS layer alone could not completely insulate the electrolyte solutions from the bottom electrode but it could be used to form a defect free underlayer for SOG film which could be used as a main electrical insulator. For instance, when a droplet of 1% KCl solution was used (instead of DI water), the generation of bubbles and the leaky current were observed on the single layer of PDMS or SOG, while those were not observed on the SOG/PDMS layer.

Prior to the deposition of the insulating layer the substrate was cleaned via AMD (acetone, methanol and DI water) or RCA cleaning step. In order to maximize the efficiency of the EWOD the insulating layer must be kept thin while maintaining the function of electrical insulator. The PDMS (monomer mixed with curing agent with a weight ratio of 10 to 1) was diluted in toluene (volume ratio of 1 to 3) and spin-coated at 6000 rpm for 10 min to suppress the effect of residual surface defects [25]. Then SOG was coated at 3000 rpm for 40 s to form a leak-free electrical insulating layer which could withstand relatively high EWOD voltages (Fig. 1a). Direct EWOD in which the voltage is directly applied to a droplet on the substrate was used to test the insulating layer. An ohmic resistor of 1 MΩ was connected in series with the EWOD substrate. The large resistor protects the system against any short circuit and at the same time could be used to measure the current. Since the resistance is large, any small leakage current due to the defects in the insulating layer will result in a large voltage drop in the resistor and could be easily detected.

The hydrophobic layer on top of the insulating layer increases the contact angle and therefore increases the pressure inside the liquid due to the increased liquid–air surface curvature. This is one of the major design considerations in our device in which the accessible range of contact angle is enhanced before applying the electric

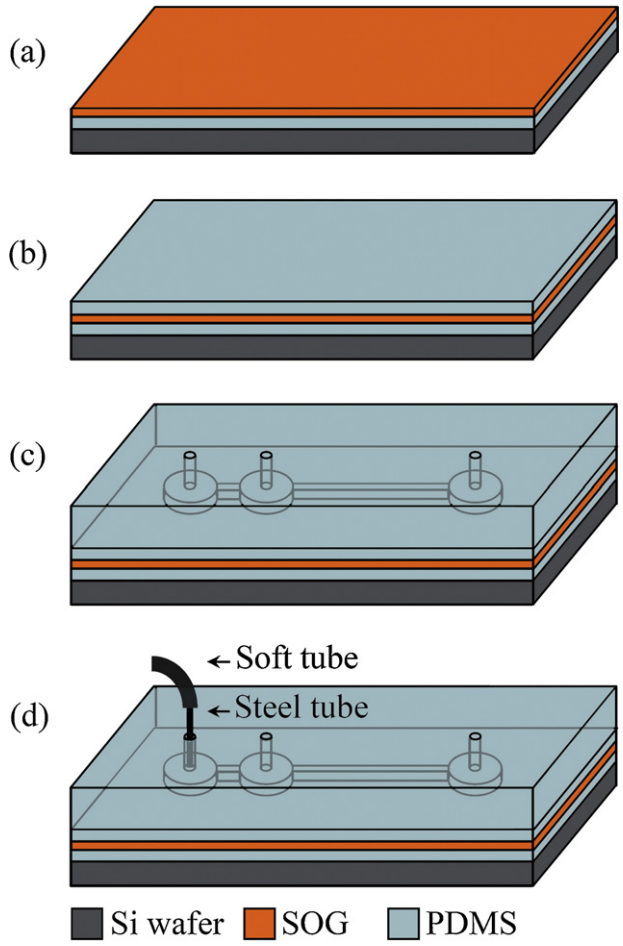

Fig. 1. Fabrication steps for the micropump. (a) Silicon wafer was used as the bottom electrode. Diluted PDMS was spin-coated to mask the defects. A SOG film was formed as an insulating layer. (b) Diluted PDMS was spin-coated again to form a thin hydrophobic film. (c) A PDMS block was cast using a SU-8 mold to form microchannels. The liquid inlet, the air outlet and the drop formation hole were punched in the PDMS block. The PDMS block with microchannels was bonded to the PDMS film. (d) The interconnection and the electrical contacts were made.

potential [26]. The hydrophobic layer from this point of view puts the meniscus in a non-wetting state ready to be relaxed and actuated by applying the voltage. In order to reduce the total material cost and simplify the fabrication steps, instead of commonly used hydrophobic materials in EWOD such as CYTOP (Asahi Glass Co.), or Teflon AF (DuPont), a second PDMS film was formed as both the hydrophobic and the bonding layer in our device (Fig. 1b).

2.2. Soft lithography and bonding

A separate PDMS block was cast using a SU-8 mold and attached to the EWOD substrate to form a microchannel. In addition to an inlet and an outlet (an escape route for air), an orifice for droplet formation was punched into the PDMS block before bonding. The fully cured PDMS thin film which was formed as the hydrophobic layer in previous step was used as the bonding layer as well. A corona discharge method [27] was used at room temperature and atmospheric pressure. A leak free bonding for fluids between the PDMS film and the microchannel block was ensured before testing (Fig. 1c).

This method is in contrast with the other methods using partially cured or uncured PDMS adhesive or a variation of cross linker for bonding. This provides the uniformity of surface characteristic to all the channel walls. It is worth mentioning that although the PDMS thin film, initially becomes hydrophilic due to the corona discharge process but this effect is not permanent and it eventually reverts to the original hydrophobic state [28,29].

2.3. Microfluidic interconnections and electrical contacts

A metallic tube with a diameter of slightly larger than the size of the punched holes in the PDMS block was inserted into the liquid inlet. The PDMS is elastic and could easily hold the inserted tube in its place and make a leak free connection for fluid. A flexible polymer tube was connected to the steel tube (Fig. 1d). A stainless steel tube inserted in the inlet was used as the upper electrode (Fig. 1d). This ensures that electrical contact to the liquid is always maintained. The upper electrode was grounded and the voltage was applied to the conductive layer in the EWOD substrate.

3. Results and discussion

The EWOD substrate was characterized by studying the effect of the electric potential on the droplet contact angle. The applied voltage to the liquid was varied from 0 V to 120 V and the droplet contact angle on the substrate was measured (Fig. 2). For voltages less than 34 V the contact angle is at its highest value, θ_{max}, and remains constant with an average value of 86°. As the voltage increases from 34 V the contact angle decreases. Finally for voltages above 90 V the contact angle saturates to its lowest value, θ_{min}, with an average value of 57°. In terms of operation, any applied voltage above 90 V only increases the risk of dielectric break-down.

A voltage of 100 V was selected (above 90 V and below 120 V) for the micropump operation to make sure that the device is working in the saturation region of the contact angle (Fig. 2). In other words increasing the voltage further will not improve the pump operation since the contact angle will not be reduced further. A working voltage in the saturation region will guarantee that the contact angle is not sensitive to small voltage fluctuations of the device.

The observed plateau at higher voltages is associated with the saturation of the contact angle which prevents the full wetting (zero contact angle) and limits the variation of the surface tension force. The theoretical explanations behind this saturation are still under debate and not conclusive yet. Various explanations have been given, which try to find this phenomenon's origination from trapping of electric charge, ionization of gas close to the liquid–solid

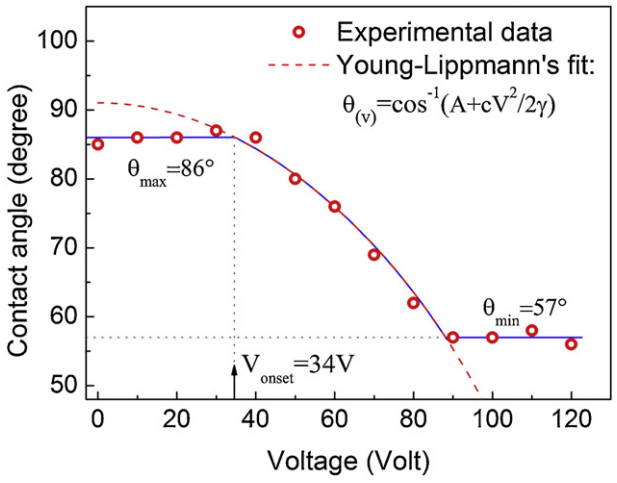

Fig. 2. Droplet contact angle on EWOD substrate vs. voltage: the dash line is the theoretical fit to the data. The hysteresis contact angle is shown as θ_{max}, the saturation contact angle is shown as θ_{min}, and the onset voltage is shown as V_{onset}. In the equation: A is a constant, c is the capacitance of the EWOD substrate and γ is the surface tension of water–air.

wetting line, wetting line instability, zero interfacial tension criterion and the droplet resistance [26,30].

On the other hand the constant value of the contact angle at lower voltages (<34 V in Fig. 2) is related to the hysteresis of the contact angle or the pinning effect [30,31]. The pinning effect is the tendency of the liquid to preserve its wetting or non-wetting states on the solid surface. This effect plays an important role at lower voltages in which EWOD is not strong enough to force the liquid to wet the hydrophobic surface.

The pinning effect tends to pin the wetting line to the surface. When an external force (e.g. due to a pressure gradient) is exerted on a wetting line, the pinning effect makes the wetting line on the surface stationary and as a result the contact angle is increased or reduced without the movement of the wetting line depending on the direction of the external force [32]. The EWOD effect tends to increase the wetted area (the contact area between the droplet and the surface) and therefore tends to reduce the contact angle. The droplet volume is constant so an increase in the wetted area means a decrease in contact angle (Eq. (3)). However, the EWOD is too weak at lower voltages and it could not move the wetting line due to the pinning effect and therefore the contact angle does not change.

The application of silicone oil to the solid surface has proved to be effective in reducing the contact angle hysteresis and improving the liquid's reaction to the change in electric potential in EWOD setup. However such surface treatment is often not desirable due to the oil residues and non-uniformity of its effect.

It is apparent that there is an onset voltage, V_{onset}, in which the contact angle starts a transition from a higher constant value to a lower constant value. The transition region could be understood using Young–Lippmann's equation [33,34] which states that the contact angle is a function of the applied voltage and the surface tensions in an electrowetting setup:

$$\theta = \cos^{-1}\left(\frac{(\gamma_{sa} - \gamma_{ls} + cV^2/2)}{\gamma_{la}}\right), \quad (1)$$

where θ is the liquid contact angle on the substrate, γ_{sa}, γ_{ls} and γ_{la} are the substrate–air, liquid–substrate and liquid–air surface tensions respectively in the absence of electric potential, V is the voltage and c is the capacitance ($\mu F/m^2$) of the EWOD substrate. Since the surface tensions are constant in this experiment, and c is constant for a specific setup, we could simplify Young–Lippmann's equation to:

$$\theta_{(V)} = \cos^{-1}(A + BV^2), \quad (2)$$

where A and B are two constants. This equation could be fitted to the experimental data using A and B as fitting parameters (dash line shown in Fig. 2). A good agreement was found between the electrowetting experimental data and the theoretical equation for voltages above 30 V and less than 90 V. The values obtained for A and B for the best fit are -1.8×10^{-2} and 7.2×10^{-5} ($1/V^2$) respectively. Using the surface tension of water–air, 72 mN/m, the capacitance of the micropump EWOD substrate, c, is obtained to be $10 \pm 0.6\ \mu F/m^2$.

The capacitance, c, and the thickness of the insulation layer, t, are related as $c = (\varepsilon_0 \varepsilon_r)/t$, where ε_0 is the vacuum permittivity and ε_r is the relative permittivity of the insulating layer. The dielectric layer in the fabricated micropump consists of a thin SOG layer and two PDMS films. The thickness of the SOG formed at 3000 rpm for 40 s is 0.2 μm. Considering the known values of relative permittivity, ε_r, of SOG and PDMS (3.9 and 2.65) and the thickness of PDMS film (1.1 μm) [25], the capacitance is calculated to be $10\ \mu F/m^2$ which is in excellent agreement with the result obtained from Young–Lippmann's equation.

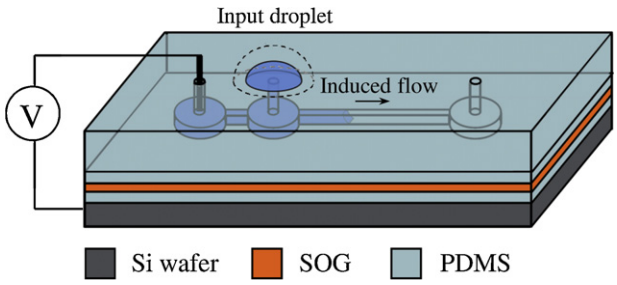

Fig. 3. The input droplet on top of the micropump is driven into the channel by applying the voltage.

Young–Lippmann's fit to the contact angle vs. voltage could be utilized to demonstrate the efficiency of EWOD setup and used as comparative measure for evaluating the strength of EWOD in one device with that in other fabricated devices. For this purpose four parameters associated with Fig. 2 are utilized: the saturation contact angle, θ_{min}, the hysteresis contact angle, θ_{max}, the capacitance of the substrate, c, and the onset voltage, V_{onset}. EWOD setup, with a larger difference between the hysteresis contact angle and the saturation contact angle, is more efficient and for a higher capacitance, c, the switching from θ_{max} to θ_{min} occurs sharply and for less change in the applied voltage (Eqs. (1) and (2)). In addition, a lower onset voltage means a lower working voltage for the device. This gives an insight into the design guideline for energy-efficient EWOD devices.

For priming, water was supplied in the channel to make contact with the hydrophobic surface of the EWOD substrate at the bottom of the channel and to form a droplet as a positive pressure source on top of the channel (Fig. 3). A liquid meniscus is also formed inside the channel. The droplet and the meniscus contact angles are in a non-wetting state on the hydrophobic PDMS surface.

Prior to applying the voltage the droplet was stable and the liquid inside the channel was in the non-wetting state (Fig. 4a and b). Only, after applying the voltage (V = 100 V), the droplet starts flowing into the channel (Fig. 4c and d). The EWOD substrate which is in contact with the liquid, works similar to a capacitor. A fringing electric field, which is formed at the substrate–liquid–air interface, helps the liquid to wet the surface and move forward in the channel. In other words the decrease in the contact angle at the bottom of the channel reduces the liquid meniscus curvature inside the channel and produces a positive pumping pressure. The droplet/meniscus pressure gradient is activated and the droplet is pumped into the channel with a uniform flow rate.

The micropump flow rate was measured to be uniform for different sizes of the droplet for the similar initial liquid length in the channel and a voltage of 100 V. Since in microfluidic devices the flow is laminar, their performance in the laminar regime is enhanced by maintaining the flow at a constant rate [9]. The result shows that regardless of reduction in the droplet size during the operation, the flow rate remains constant [35]. Nevertheless the flow rate is strongly dependent on the initial droplet size (Fig. 5a) and the higher flow rate is obtained from a smaller droplet. A smaller droplet has a higher Laplace pressure due to higher surface curvature and induces a higher flow rate inside the channel. Moreover the liquid flow rate in the channel is increased by increasing the micropump's working voltage (Fig. 5b). The meniscus contact angle on the bottom of the channel is reduced by increasing the voltage. The meniscus with lower contact angle implies a lower pressure in the channel and therefore a higher flow rate is induced.

The droplet volume vs. time could be found from the information given in Fig. 5, if the initial droplet volume is known. The change in droplet volume is equal to the change in liquid volume in the channel, which could be obtained by multiplying meniscus

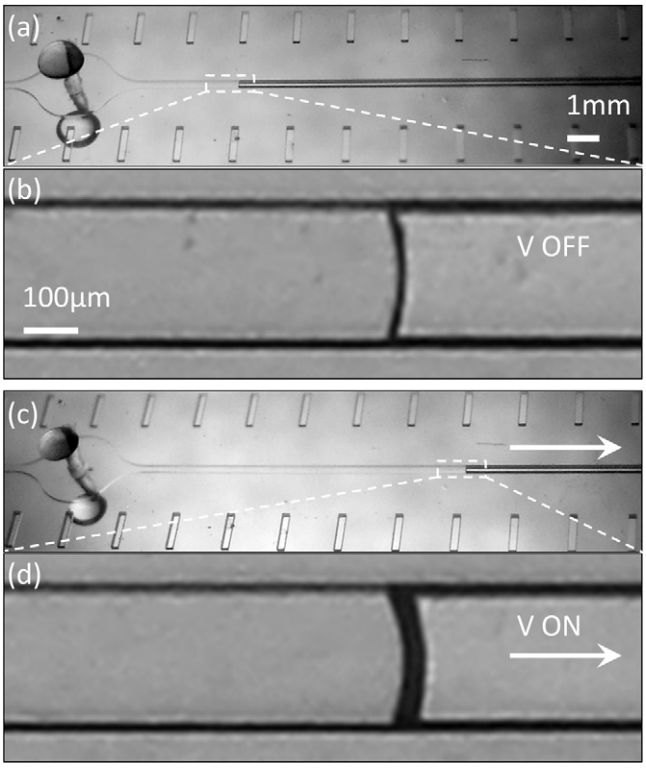

Fig. 4. The micropump in operation at 100 V (a) a slanted view of the input droplet and the meniscus before applying voltage, (b) a magnification of the same meniscus in a, observed from top, (c) a slanted view of the reduced input droplet and the advanced meniscus in the channel after applying voltage (d) the same meniscus in c, observed from top which shows the increased wetting area.

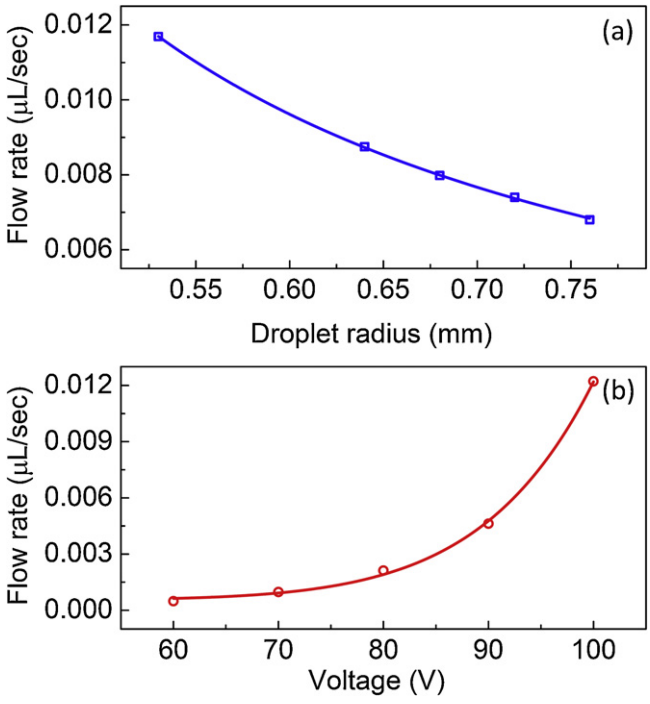

Fig. 5. The volumetric flow rate in the channel is shown as a function of (a) droplet radius at a constant voltage of 100 V and (b) voltage for a similar droplet radius of 0.5 mm.

velocity in the channel from Fig. 5 by the channel cross section area (250 μm × 100 μm). Since the meniscus velocity in the channel is constant, the droplet volume decreases linearly with time. The micropump input droplet is assumed to be a spherical cap since its radius, R_D, is less than the capillary length for a droplet, $(\gamma/4\rho g)^{1/2}$, where γ and ρ are the surface tension and the density of water respectively and g is the gravity. The droplet's initial volume could be calculated from:

$$V_{\text{droplet}} = \pi\left(\frac{a_D}{\sin\theta_D}\right)^3\left(\frac{2}{3} - \frac{\cos\theta_D}{3}(2 + (\sin\theta_D)^2\right), \quad (3)$$

where a_D is the initial droplet wetting radius and θ_D is the initial droplet contact angle (86°). Using the top view image of the droplet, the radius of wetting area, a_D, could be measured directly and is used in Eq. (3) instead of the droplet radius, R_D.

The key concept in the pump design is the utilization of the pressure gradient between the droplet and the liquid in the channel. The meniscus pressure, P_M, in the channel could be obtained from [36]:

$$P_M = -\gamma_{VL}\cdot\left(\frac{\cos\theta_{Ch}\cdot(2h+w) + \cos\theta_{EW}\cdot w}{hw}\right), \quad (4)$$

where γ_{VL} is the liquid–vapor surface tension, h and w are the height and the width of the channel, θ_{Ch} is the liquid contact angle on the channel walls, and θ_{EW} is the liquid contact angle on the bottom of the channel on which EWOD is performed. The micropump pressure gradient which is defined as the difference between the droplet pressure, P_D, $(2\gamma_{VL}/R_D)$ and the meniscus pressure, P_M is:

$$P_{\text{MP}} = \gamma_{VL}\cdot\left(\frac{2}{R_D} + \frac{\cos\theta_{Ch}\cdot(2h+w) + \cos\theta_{EW}\cdot w}{hw}\right) \quad (5)$$

The micropump pressure gradient is proportional to the liquid flow rate in the channel:

$$P_D - P_M = K_\mu\cdot L_{eff}\cdot Q, \quad (6)$$

where K is a geometrical constant, μ is the liquid viscosity, Q is the volumetric flow rate and L_{eff} is the effective liquid length in the channel (the sum of the liquid length in the channel, L_{Ch}, orifice length, and other head losses).

The micropump pressure predicted by Eq. (5) depends on the accurate estimation of θ_{Ch} and θ_{EW}. When the EWOD valve is switching from off to on, θ_{Ch} is equal to the maximum advancing contact angle at zero velocity which was measured to be 100° [35]. The θ_{EW} (Fig. 2) was scaled from 86° to 100° at zero voltage to account for the advancing contact angle.

A MATLAB code was written using Eqs. (4) and (5) and the voltage dependence of θ_{EW} to predict the micropump driving pressure at different voltages and for various droplet sizes (Fig. 6). The input droplet radius and the voltage are used to plot the driving pressure of the micropump in a 3D graph (Fig. 6a). The constant pressure contours, including the zero pressure line, are shown on the surface. The EWOD valve will be opened and a flow will be induced in the channel for a combination of voltage and R_D for which the pressure is positive (red region in Fig. 6a). The valve remains closed if the pressure is negative (blue region in Fig. 6a).

For a constant R_D of 0.7 mm (white dashed line) the pump pressure crosses the zero value as the working voltage increases (Fig. 6a and b). It is shown that for a very small droplet radius, such as 0.2 mm, the pump pressure is always positive and valve is open, even without applying voltage. In other words the surface curvature of small droplets is high enough to drive the pump by means of a high Laplace pressure inside the droplet.

Also for a constant voltage (white dot-dashed line), the pump pressure crosses the zero value as the radius of the input droplet increases (Fig. 6a and c). For a range of droplet sizes in region I

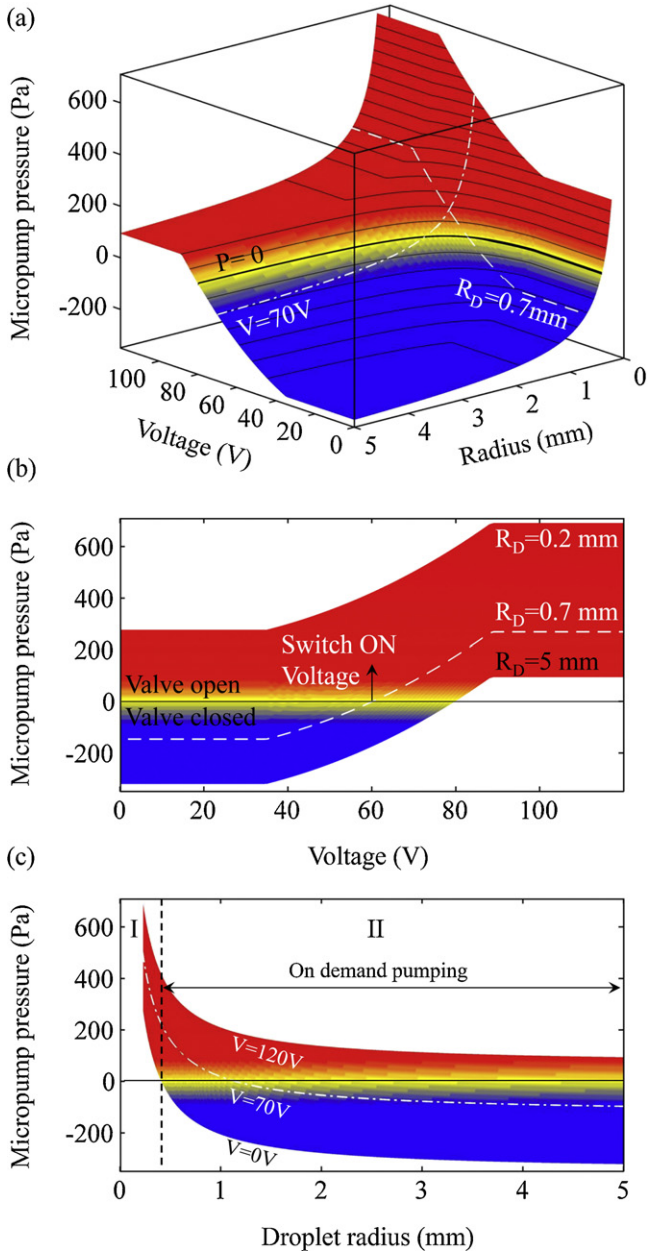

Fig. 6. The outputs of MATLAB code showing the micropump pressure as a function of voltage and droplet radius (a) 3D representation, (b) voltage effect highlighted for R_D = 5, 0.7 and 0.2 mm, (c) droplet radius effect highlighted for V = 0, 70 and 120 V. (For interpretation of the references to color in the text, the reader is referred to the web version of the article.)

(Fig. 6c) the valve will be always open without applying voltage. In the region II at zero voltage the valve is closed and by increasing the voltage it will switch to be open. Therefore region II represents the range of R_D for which the droplets are pumped on-demand. Further increasing the voltage will increase the pressure and induce a higher flow rate in the channel.

Eq. (6) shows a direct relation between the micropump driving pressure, P_{MP} and the flow rate in the channel. The code outputs for micropump pressure, shown in Fig. 6b and c, strongly correlate with the flow rate data presented in Fig. 5a and b. The flow rate decreases by increasing the size of the input droplet and increases by increasing the voltage (Fig. 5). This observation correlates with the predicted micropump pressure (Eq. (6)) which shows the same trend by altering the input droplet size and the voltage.

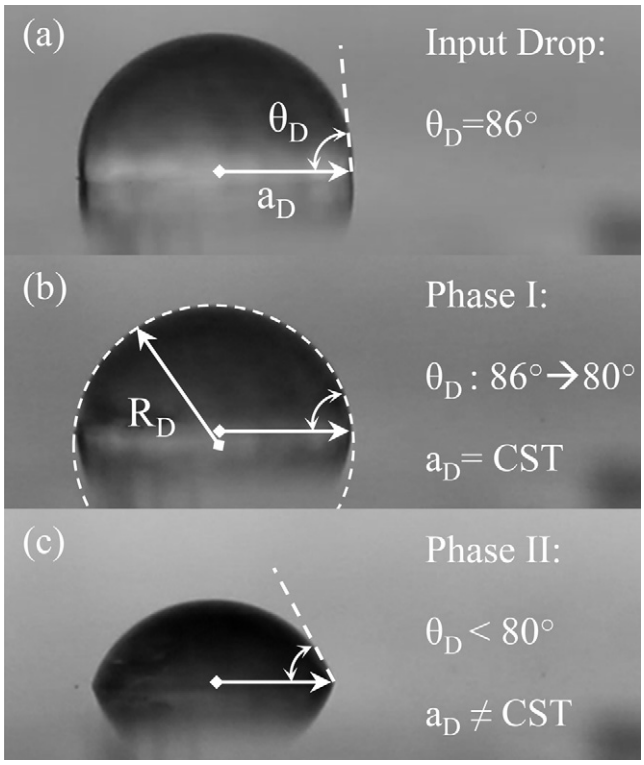

Fig. 7. Droplet pumping phases in which R_D is surface radius of curvature and a_D is droplet wetting radius. (a) Stable droplet on top of the PDMS channel with an initial contact angle, θ_D, of 86° prior to applying voltage. (b) Phase I: a_D is constant while θ_D decreases. (c) phase II: both a_D and θ_D decrease.

After the pump switches on by applying the voltage, droplet shrinks in two phases: in phase one, the droplet wetting area remains constant as the contact angle is reduced to 80° (Fig. 7a and b). In phase two, both the droplet wetting area and the contact angle decrease (Fig. 7b and c). Several models are proposed in the past to describe different phases of a shrinking droplet [37–40]. However, the comparison of the different models reveals that a generally accepted model has not been developed yet. In general, the different observations could be attributed to different experimental conditions.

By observing the gradually evaporating droplets on a solid surface, two modes are described [37]. In the first mode the contact angle is decreasing with a constant wetting area (CWA) and in the second mode the wetting area decreases with a constant contact angle (CCA). Birdi and Vu have described the shrinkage of the water drop as a single phase phenomenon [38] (attributed to the pinning effect) in which depending on the initial value of the contact angle, only one of the two modes mentioned above takes place: CWA for solid surfaces with wetting characteristics, such as glass ($\theta_D < 90°$) and CCA for surfaces with nonwetting characteristics such as Teflon ($\theta_D > 90°$).

McHale et al. suggested a two phases model [39]. The first phase is similar to the previous model [38] for both hydrophilic and hydrophobic surfaces. However in the second phase both the contact angle and the wetting area are changing though the evaporation time scale is dominated by the first phase. This is due to the increasing rate of reduction of the contact radius and the velocity dependence of the contact angle. Yu et al. also have reported a two phases model [40]. However their model does not depend on the initial contact angle. It always starts from CWA and switches to CCA. This model is identical to the model used to describe the shrinkage of a passively pumped droplet by a surface tension based pumping method [9].

Our observations are in relatively good agreement with McHale et al. [39], although due to the micropump's higher flow rate the second phase is much more pronounced. This is the major difference between our experiment and evaporating droplets. The concurrent decrease of the droplet's contact angle and wetting area is also observed in the forced wetting [41] in which the droplet wetting area is forced to move by application of an external effect, such as a pressure gradient in the micropump. In such case the contact angle depends on the velocity of the wetting line, and by changing the velocity the contact angle is changed [35].

4. Conclusions

The pressure gradient induced between the droplet and the meniscus in the channel was used to design a constant flow rate micropump with no moving parts for pumping non-electrolyte aqueous solutions. Altering the surface tension by changing the electric potential in EWOD was introduced as an efficient and low power consumption propellant method which provides on demand flow on/off capability. The efficiency and the strength of the EWOD substrate were evaluated using four parameters: capacitance, hysteresis contact angle, saturation contact angle, and onset voltage. The micropump was prepared using one mask fabrication process and could be operated at preset voltage.

The EWOD valve switch on voltages for various droplet sizes and the range of droplet radii for on demand pumping were depicted. The predicted driving pressure from the EWOD valve model correlated to the measured data for the liquid flow rate in the channel.

A model based on the forced wetting was developed for describing the behavior of the actuated input droplet. In the first phase the droplet wetting area is constant while contact angle is decreasing and in the second phase the droplet contact angle and wetting area are decreasing simultaneously. The developed micropump in this work is simple in its design and fabrication and yet provides the on-demand supply function with much desired features such as short response time, low power consumption, no fluid leakage, no dead volume, disposability and biocompatibility.

Acknowledgements

This work was partially supported by National Science Foundation, USA (ECCS 0901503), NRF WCU Program, Korea (R32-2008-000-10124-0) and Korea Electrotechnology Research Institute (KERI) under the Ministry of Knowledge Economy (12-12-N0201-09), Korea.

References

[1] K.W. Oh, C.H. Ahn, A review of microvalves, Journal of Micromechanics and Microengineering 16 (2006) R13–R39.
[2] D.J. Laser, J.G. Santiago, A review of micropumps, Journal of Micromechanics and Microengineering 14 (2004) R35–R64.
[3] B. Iverson, S. Garimella, Recent advances in microscale pumping technologies: a review and evaluation, Microfluidics and Nanofluidics 5 (2008) 145–174.
[4] A. Nisar, N. Afzulpurkar, B. Mahaisavariya, A. Tuantranont, MEMS-based micropumps in drug delivery and biomedical applications, Sensors and Actuators B: Chemical 130 (2008) 917–942.
[5] F. Amirouche, Y. Zhou, T. Johnson, Current micropump technologies and their biomedical applications, Microsystem Technologies 15 (2009) 647–666.
[6] N.C. Tsai, C.Y. Sue, Review of MEMS-based drug delivery and dosing systems, Sensors and Actuators A: Physical 134 (2007) 555–564.
[7] J.K. Luo, Y.Q. Fu, Y. Li, X.Y. Du, A.J. Flewitt, A.J. Walton, W.I. Milne, Moving-part-free microfluidic systems for lab-on-a-chip, Journal of Micromechanics and Microengineering 19 (2009) 054001.
[8] S.Y. Xing, R.S. Harake, T.R. Pan, Droplet-driven transports on superhydrophobic-patterned surface microfluidics, Lab on a Chip 11 (2011) 3642–3648.
[9] E. Berthier, D.J. Beebe, Flow rate analysis of a surface tension driven passive micropump, Lab on a Chip 7 (2007) 1475–1478.
[10] J. Lee, C.J. Kim, Surface-tension-driven microactuation based on continuous electrowetting, Journal of Microelectromechanical Systems 9 (2000) 171–180.
[11] S.K. Cho, H. Moon, C.-J. Kim, Creating, transporting, cutting, and merging liquid droplets by electrowetting-based actuation for digital microfluidic circuits, Journal of Microelectromechanical Systems 12 (2003) 70–80.
[12] H. Ren, R.B. Fair, M.G. Pollack, E.J. Shaughnessy, Dynamics of electro-wetting droplet transport, Sensors and Actuators B: Chemical 87 (2002) 201–206.
[13] H. Ren, R.B. Fair, M.G. Pollack, Automated on-chip droplet dispensing with volume control by electro-wetting actuation and capacitance metering, Sensors and Actuators B: Chemical 98 (2004) 319–327.
[14] J. Lee, H. Moon, J. Fowler, T. Schoellhammer, C.-J. Kim, Electrowetting and electrowetting-on-dielectric for microscale liquid handling, Sensors and Actuators A: Physical 95 (2002) 259–268.
[15] T. Pan, S.J. McDonald, E.M. Kai, B. Ziaie, A magnetically driven PDMS micropump with ball check-valves, Journal of Micromechanics and Microengineering 15 (2005) 1021–1026.
[16] K.-S. Yun, I.-J. Cho, J.-U. Bu, G.-H. Kim, Y.-S. Jeon, C.-J. Kim, E. Yoon, A micropump driven by continuous electrowetting actuation for low voltage and low power operations, in: The 14th IEEE International Conference on Micro Electro Mechanical Systems, 2001, MEMS 2001, 2001, pp. 487–490.
[17] Z. Fekete, P. Nagy, G. Huszka, F. Tolner, A. Pongrácz, P. Fürjes, Performance characterization of micromachined particle separation system based on Zweifach–Fung effect, Sensors and Actuators B: Chemical 162 (2012) 89–94.
[18] M. Kersaudy-Kerhoas, R. Dhariwal, M.P.Y. Desmulliez, L. Jouvet, Hydrodynamic blood plasma separation in microfluidic channels, Microfluidics and Nanofluidics 8 (2010) 105–114.
[19] S. Yang, A. Undar, J.D. Zahn, A microfluidic device for continuous, real time blood plasma separation, Lab on a Chip 6 (2006) 871–880.
[20] E. Sollier, M. Cubizolles, Y. Fouillet, J.L. Achard, Fast and continuous plasma extraction from whole human blood based on expanding cell-free layer devices, Biomedical Microdevices 12 (2010) 485–497.
[21] A.I. Rodriguez-Villarreal, M. Arundell, M. Carmona, J. Samitier, High flow rate microfluidic device for blood plasma separation using a range of temperatures, Lab on a Chip 10 (2010) 211–219.
[22] M. Kersaudy-Kerhoas, D.M. Kavanagh, R.S. Dhariwal, C.J. Campbell, M.P.Y. Desmulliez, Validation of a blood plasma separation system by biomarker detection, Lab on a Chip 10 (2010) 1587–1595.
[23] A. Lenshof, A. Ahmad-Tajudin, K. Jaras, A.M. Sward-Nilsson, L. Aberg, G. Marko-Varga, J. Malm, H. Lilja, T. Laurell, Acoustic whole blood plasmapheresis chip for prostate specific antigen microarray diagnostics, Analytical Chemistry 81 (2009) 6030–6037.
[24] J.S. Go, S. Shoji, A disposable, dead volume-free and leak-free in-plane PDMS microvalve, Sensors and Actuators A 114 (2004) 438–444.
[25] J.H. Koschwanez, R.H. Carlson, D.R. Meldrum, Thin PDMS films using long spin times or tert-butyl alcohol as a solvent, PLoS ONE 4 (2009) e4572.
[26] A. Quinn, R. Sedev, J. Ralston, Contact angle saturation in electrowetting, The Journal of Physical Chemistry B 109 (2005) 6268–6275.
[27] K. Haubert, T. Drier, D. Beebe, PDMS bonding by means of a portable, low-cost corona system, Lab on a Chip 6 (2006) 1548–1549.
[28] H. Hillborg, U.W. Gedde, Hydrophobicity recovery of polydimethylsiloxane after exposure to corona discharges, Polymer 39 (1998) 1991–1998.
[29] J. Kim, M.K. Chaudhury, Corona-discharge-induced hydrophobicity loss and recovery of silicones, in: Annual Report Conference on Electrical Insulation and Dielectric Phenomena, 1999, vol. 702, 1999, pp. 703–706.
[30] D. Brassard, L. Malic, F. Normandin, M. Tabrizian, T. Veres, Water-oil core-shell droplets for electrowetting-based digital microfluidic devices, Lab on a Chip 8 (2008) 1342–1349.
[31] J. Berthier, P. Dubois, P. Clementz, P. Claustre, C. Peponnet, Y. Fouillet, Actuation potentials and capillary forces in electrowetting based microsystems, Sensors and Actuators A: Physical 134 (2007) 471–479.
[32] R. Tadmor, Line energy and the relation between advancing, receding, and Young contact angles, Langmuir 20 (2004) 7659–7664.
[33] G. Lippmann, Relation entre les phenomenes electriques et capillaires, Annales de Chimie et de Physique 5 (1875) 494–549.
[34] T. Young, An essay on the cohesion of fluids, Philosophical Transactions of the Royal Society of London 95 (1805) 65–87.
[35] R. Shabani, H.J. Cho, A micropump controlled by EWOD: wetting line energy and velocity effects, Lab on a Chip 11 (2011) 3401–3403.
[36] K. Hosokawa, T. Fujii, I. Endo, Droplet-based nano/picoliter mixer using hydrophobic microcapillary vent, in: Twelfth IEEE International Conference on Micro Electro Mechanical Systems, 1999, MEMS '99, 1999, pp. 388–393.
[37] R.G. Picknett, R. Bexon, Evaporation of sessile or pendant drops in still air, Journal of Colloid and Interface Science 61 (1977) 336–350.
[38] K.S. Birdi, D.T. Vu, Wettability and the evaporation rates of fluids from solid-surfaces, Journal of Adhesion Science and Technology 7 (1993) 485–493.
[39] G. McHale, S.M. Rowan, M.I. Newton, M.K. Banerjee, Evaporation and the wetting of a low-energy solid surface, The Journal of Physical Chemistry B 102 (1998) 1964–1967.
[40] H.-Z. Yu, D.M. Soolaman, A.W. Rowe, J.T. Banks, Evaporation of water microdroplets on self-assembled monolayers: from pinning to shrinking, ChemPhysChem 5 (2004) 1035–1038.
[41] T.D. Blake, The physics of moving wetting lines, Journal of Colloid and Interface Science 299 (2006) 1–13.

Biographies

Roxana Shabani is working as a research assistant in the Nanofab and BioMEMS Lab in University of Central Florida. She is a Ph.D. student majoring in mechanical engineering in the department of Mechanical, Materials and Aerospace Engineering at UCF. She earned her B.Sc. in mechanical engineering from the University of Tehran in 2007. She is currently working on computational modeling and experimentation of the wetting line energy and velocity effects on liquid flow in microfluidic devices. Her research interests include design and fabrication of droplet based microfluidic systems, and microfluidic transport using electrowetting on dielectric (EWOD).

Hyoung J. Cho is an associate professor in the Department of Mechanical, Materials and Aerospace Engineering at the University of Central Florida. He is currently the director of the NanoFab and BioMEMS Lab at the UCF. He earned his Ph.D. in Electrical Engineering from University of Cincinnati (USA) in 2002, and MS and BS in Materials Engineering from Seoul National University (Korea) in 1991 and 1989, respectively. His current research interests include surface tension-driven microfluidic components, nanoparticle-integrated gas sensors, and micromachined electrochemical sensors for ROS (reactive oxygen species) detection. He was a recipient of NSF CAREER award in 2004.